AFRL-VA-WP-TP-2006-329

A RAPID ASSESSMENT TOOL FOR SPACE ACCESS VEHICLE CONFIGURATIONS IN GUIDANCE AND CONTROL PERFORMANCE (PREPRINT)

Anhtuan D. Ngo, Michael W. Oppenheimer,
William B. Blake, and Gregory E. Moster

AUGUST 2006

Approved for public release; distribution is unlimited.

STINFO COPY

AIR VEHICLES DIRECTORATE
AIR FORCE MATERIEL COMMAND
AIR FORCE RESEARCH LABORATORY
WRIGHT-PATTERSON AIR FORCE BASE, OH 45433-7542

NOTICE AND SIGNATURE PAGE

AFRL-VA-WP-TP-2006-329 HAS BEEN REVIEWED AND IS APPROVED FOR PUBLICATION IN ACCORDANCE WITH ASSIGNED DISTRIBUTION STATEMENT.

*//Signature//

Anhtuan D. Ngo
Aerospace Engineer
Control Design and Analysis Branch
Air Force Research Laboratory
Air Vehicles Directorate

//Signature//

Brian J. Gamble
Deputy Chief
Control Design and Analysis Branch
Air Force Research Laboratory
Air Vehicles Directorate

//Signature//

JEFFREY C. TROMP
Senior Technical Advisor
Control Sciences Division
Air Vehicles Directorate

This report is published in the interest of scientific and technical information exchange, and its publication does not constitute the Government's approval or disapproval of its ideas or findings.

*Disseminated copies will show "//Signature//" stamped or typed above the signature blocks.

REPORT DOCUMENTATION PAGE

Form Approved
OMB No. 0704-0188

1. REPORT DATE *(DD-MM-YY)*	2. REPORT TYPE	3. DATES COVERED *(From - To)*
August 2006	Conference Paper Preprint	08/08/2005– 08/08/2006

4. TITLE AND SUBTITLE

A RAPID ASSESSMENT TOOL FOR SPACE ACCESS VEHICLE CONFIGURATIONS IN GUIDANCE AND CONTROL PERFORMANCE (PREPRINT)

5a. CONTRACT NUMBER
In-house

5b. GRANT NUMBER

5c. PROGRAM ELEMENT NUMBER
602201F

6. AUTHOR(S)

Anhtuan D. Ngo, Michael W. Oppenheimer, and William B. Blake (AFRL/VACA)
Gregory E. Moster (AFRL/VASD)

5d. PROJECT NUMBER
N/A

5e. TASK NUMBER
N/A

5f. WORK UNIT NUMBER
N/A

7. PERFORMING ORGANIZATION NAME(S) AND ADDRESS(ES)

Control Design and Analysis Branch (AFRL/VACA)
Structural Design and Analysis Branch (AFRL/VASD)
Control Sciences Division
Air Vehicles Directorate
Air Force Materiel Command, Air Force Research Laboratory
Wright-Patterson Air Force Base, OH 45433-7542

8. PERFORMING ORGANIZATION REPORT NUMBER
AFRL-VA-WP-TP-2006-329

9. SPONSORING/MONITORING AGENCY NAME(S) AND ADDRESS(ES)

Air Vehicles Directorate
Air Force Research Laboratory
Air Force Materiel Command
Wright-Patterson Air Force Base, OH 45433-7542

10. SPONSORING/MONITORING AGENCY ACRONYM(S)
AFRL-VA-WP

11. SPONSORING/MONITORING AGENCY REPORT NUMBER(S)
AFRL-VA-WP-TP-2006-329

12. DISTRIBUTION/AVAILABILITY STATEMENT
Approved for public release; distribution is unlimited.

13. SUPPLEMENTARY NOTES

This work has been submitted to the Proceedings of the AIAA Space 2006 Conference and Exhibit.

PAO Case Number: AFRL/WS 06-1949 (cleared August 19, 2006).

14. ABSTRACT

A guidance and control (G\&C) design tool to rapidly assess the necessary control effort of a conceptual space access vehicle to track its flight trajectory is described. This tool can be used as part of the preliminary design cycle in configuration, trajectory planning, structural analysis, aerodynamic modeling, and control surface sizing. Given a conceptual configuration for a space access vehicle and a desired trajectory for a reentry flight, this G\&C tool provides an inner-loop feedback control law and outer loop feedback guidance law to track the given trajectory. Assessment of the vehicle's tracking performance and associated aero-control usage can be made. This assessment can then be used to determine the appropriate control.

15. SUBJECT TERMS

16. SECURITY CLASSIFICATION OF:			17. LIMITATION OF ABSTRACT:	18. NUMBER OF PAGES	19a. NAME OF RESPONSIBLE PERSON (Monitor)
a. REPORT	b. ABSTRACT	c. THIS PAGE			Anhtuan D. Ngo
Unclassified	Unclassified	Unclassified	SAR	28	19b. TELEPHONE NUMBER *(Include Area Code)* N/A

Standard Form 298 (Rev. 8-98)
Prescribed by ANSI Std. Z39-18

A Rapid Assessment Tool for Space Access Vehicle Configurations in Guidance and Control Performance

Anhtuan D. Ngo*, Michael W. Oppenheimer*, William B. Blake†, Gregory E. Moster‡

Air Force Research Laboratory

Wright-Patterson AFB, OH 45433

A guidance and control (G&C) design tool to rapidly assess the necessary control effort of a conceptual space access vehicle to track its flight trajectory is described. This tool can be used as part of the preliminary design cycle in configuration, trajectory planning, structural analysis, aerodynamic modeling, control surface sizing. Given a conceptual configuration for a space access vehicle and a desired trajectory for a reentry flight, this G&C tool provides an inner loop feedback control law and outer loop feedback guidance law to track the given trajectory. The inner loop control law, based on dynamic inversion with a non-linear control allocator, is used to linearize the vehicle dynamics over its flight envelope and assign control tasks over the available control effectors to track the desired roll rate P, pitch rate Q, and yaw rate R. The outer-loop guidance law is based on backstepping method that transforms the trajectory-related flight path angle γ and desired bank angle ϕ into commands in roll rate P_{comd}, pitch rate Q_{comd}, and yaw rate R_{comd}. Assessment of the vehicle's tracking performance and associated aero-control usage can be made. This assessment can then be used to determine the appropriate control sizing, and mass properties for the vehicle.

*Electronic Engineer, Control Design and Analysis Branch, Air Vehicles Directorate, and AIAA Member.

†Aerospace Engineer, Control Design and Analysis Branch, Air Vehicles Directorate, and AIAA Associate Fellow.

‡Aeronautical Engineer, Structural Design and Analysis Branch, Air Vehicles Directorate, and AIAA Member.

I. INTRODUCTION

During the space access vehicle preliminary design process, it is necessary to quickly and economically assess the vehicle's ability to track a given trajectory utilizing aerodynamic and propulsion control effectors. This paper details a framework that efficiently incorporates the space access vehicle's stability, guidance and control considerations into the initial configuration development. In this approach, a well-known, high-fidelity trajectory generator (Program to Optimize Simulated Trajectories), a fast aerodynamic data computation algorithm (Missile Datcom), and a robust, large flight envelope control law are integrated in the analysis and assessment process to evaluate vehicle performance in stability, guidance, and control. POST (Program to Optimize Simulated Trajectories) is a trajectory computation program developed by NASA-Langley in 1970's to support the Space Shuttle program. POST finds a user-defined optimal trajectory based upon a simulation model with performance and loading constraints. This optimal trajectory is a compromise between the ascent phase trying to maximize the payload delivered to orbit, the entry phase trying to limit re-entry aerodynamic heating and structural loads, and the approach phase trying to prepare the vehicle for a successful landing. The ascent phase ends at stage separation which is defined as a velocity of $7,000$ feet per second, a flight path angle of 20 degrees, an angle of attack of 0 degrees, and an altitude higher than $160,000$ feet. During this phase the vehicle is ascending rapidly, passing through the transonic sound barrier, and trying to reach stage separation criteria. Flight loads are constrained or limited to a dynamic pressure of less than 800 pounds per square foot, body axial loads less than 6 g's, and body normal loads less than 3.5 g's. The entry phase begins at stage separation and ends near the landing site which is defined to be an altitude greater than $15,000$ feet and a velocity greater than Mach 0.3. During this phase the vehicle typically experiences the peak heating, dynamic pressure, and normal loads because the vehicle is ballistic and aerodynamic controls are ineffective. In this phase the vehicle will descend at a constant angle of attack of 35 degrees and then perform a pull-up maneuver to intercept a constant flight-path angle glide of 12 degrees. The imposed constraints are the same dynamic pressure, axial g, and normal g loads cited above. Heating constraints are not enforced because temperatures estimates are calculated using MINIVER off-line. The heat flux or heat rate estimates calculated in POST are used for reference only and "ball-park" approximation.

The POST simulation model consists of a rocket engine model, an aerodynamic model, mass model,

atmosphere model, and Earth gravity model. All of these models are combined to estimate the forces and moments exerted upon the vehicle over time. Typically, POST trajectories use three degrees of freedom to solve the optimization problem; therefore, losses due to trim effects are not considered and control effectors are not sized appropriately. In some cases vehicles may appear to "close" (correctly sized in terms of required fuel and subsystems) that are actually not closed and may not be closeable (fuel and subsystem growth rate is too high). Therefore, accurate sizing makes six degree of freedom (6 DOF) simulations a vital part of vehicle design process. Additionally, the 6 DOF simulations provide higher fidelity results that can be used to impact other subsystems such as the thermal protection system, main rocket engine thrust, and main propellant tank volume.

POST finds a user-defined optimal trajectory based upon a simulation model with performance and loading constraints. This optimal trajectory is a compromise between the ascent phase trying to maximize the payload delivered to orbit, the entry phase trying to limit re-entry aerodynamic heating and structural loads, and the approach phase trying to prepare the vehicle for a successful landing. The ascent phase ends at stage separation which is defined as a velocity of 7,000 feet per second, a flight path angle of 20 degrees, an angle of attack of 0 degrees, and an altitude higher than 160,000 feet. During this phase the vehicle is ascending rapidly, passing through the transonic sound barrier, and trying to reach stage separation criteria. Flight loads are constrained or limited to a dynamic pressure of less than 800 pounds per square foot, body axial loads less than 6 g's, and body normal loads less than 3.5 g's. The entry phase begins at stage separation and ends near the landing site which is defined to be an altitude greater than 15,000 feet and a velocity greater than Mach 0.3. During this phase the vehicle typically experiences the peak heating, dynamic pressure, and normal loads because the vehicle is ballistic and aerodynamic controls are ineffective. In this phase the vehicle will descend at a constant angle of attack of 35 degrees and then perform a pull-up maneuver to intercept a constant flight-path angle glide of 12 degrees. The imposed constraints are the same dynamic pressure, axial g, and normal g loads cited above. Heating constraints are not enforced because temperatures estimates are calculated using MINIVER off-line. The heat flux or heat rate estimates calculated in POST are used for reference only and "ball-park" approximation.

The POST simulation model consists of a rocket engine model, an aerodynamic model, mass model, atmosphere model, and Earth gravity model. All of these models are combined to estimate the forces and

moments exerted upon the vehicle over time. Typically, POST trajectories use three degrees of freedom to solve the optimization problem; therefore, losses due to trim effects are lost and control effectors are not sized appropriately. In some cases vehicles may appear to "close" (correctly sized in terms of required fuel and subsystems) that are actually not closed and may not be closeable (fuel and subsystem growth rate is too high). Therefore, accurate sizing makes six degree of freedom (6 DOF) simulations a vital part of vehicle design process. Additionally, the 6 DOF simulations provide higher fidelity results that can be used to impact other subsystems such as the thermal protection system, main rocket engine thrust, and main propellant tank volume.

The aerodynamic data of the vehicle can be obtained from Missile Datcom which is a tool to rapidly estimate the aerodynamics of a wide variety of vehicle configurations. The predictive accuracy of Datcom is adequate for preliminary designs. Iterations on the vehicle configurations are inevitable since the ultimate shape of the vehicle will be dependent upon the subsystem being utilized, such as payload size, propulsion method, launch and landing configurations. Once the optimal trajectory has been calculated by POST for a given vehicle configuration having the aerodynamic properties indicated by DATCOM, the task of stabilizing the vehicle and tracking the optimal trajectory is carried out by a control law. The control law is designed for the flight envelope and can accommodate the drastic change in speed, altitude, and vehicle's mass properties during ascent and reentry. These changes in the flight environment result in substantial variations in aero-dynamic pressure, stagnation temperature, center of gravity, and moments of inertia. Furthermore, the launch vehicle is powered by a propulsion system during its ascent and, for a reusable vehicle, may be unpowered during reentry. The vehicle's launch configuration and landing configuration may also be different from each other. The novel control law seeks to stabilize the vehicle and track an optimal trajectory without the lengthy design process or a complicated control law gain scheduling that is traditionally required. The inputs to the inner-loop control law are the commanded roll rate P_{comd}, commanded pitch rate Q_{comd}, and commanded yaw rate R_{comd}. The guidance and control interface translates the bank angle command and angle of attack command into the commanded roll, pitch and yaw rates P_{comd}, Q_{comd}, R_{comd} respectively. Using the output of the control law, the vehicle designer can assess vehicle performance in tracking the desired trajectory and make modifications to its configuration, if necessary. The design process is shown in Figure 1.

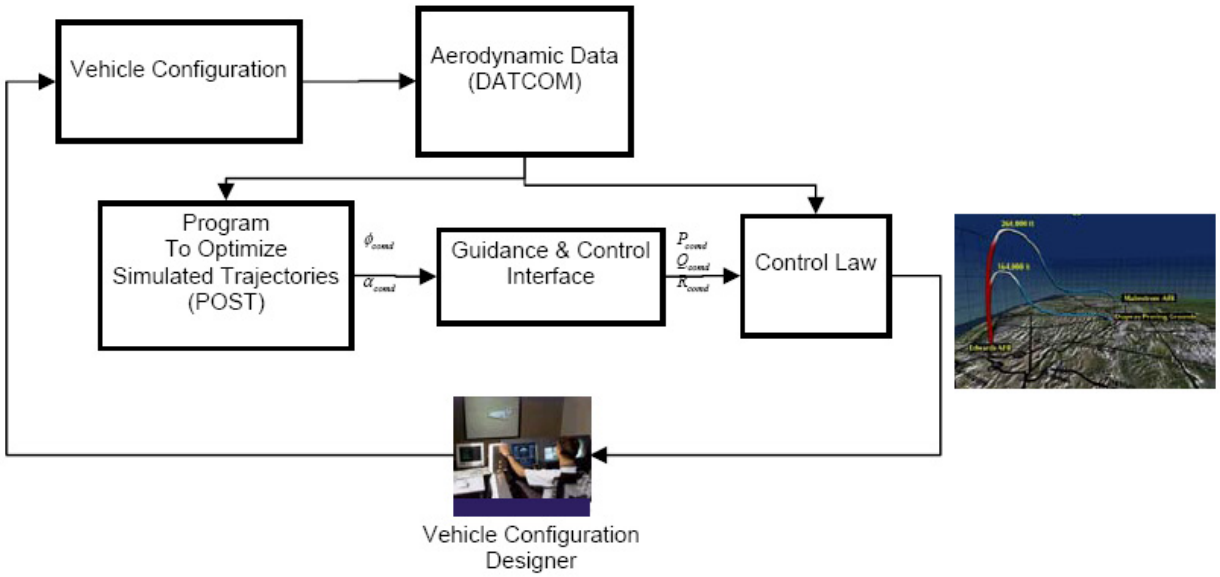

Figure 1. Space Access Vehicle's Preliminary Design Cycle

II. Vehicle Modeling

The preliminary configuration for baseline space access vehicle is shown in Figure 2. The body as modeled by Missile Datcom consists of a blunted nose followed by a cylindrical afterbody with a 17 ft diameter. A single body flap was modelled at the base of the body. There was no modelling of external rocket nozzles. A straked wing with an outer panel sweep of 42° was modelled. Vertical tails were placed on each wingtip. Five control devices were modelled, two rudders (one on each vertical tail), two elevons (one on each wing) and a body flap. The chord of the rudders was assumed to be 0.30 of the local chord. The chord of the elevons varied linearly from 0.20 of the wing root to 0.50 of the wing tip. As defined, the wing root is 20.4 ft and does not include the strake. Missile Datcom[1] was used to calculate the aerodynamic characteristics of the vehicle. Missile Datcom is a widely used engineering level code that uses the component buildup technique to predict vehicle characteristics. Code input consists of body, wing and tail geometry, Mach number, altitude, angle of attack and control deflections. Control devices are limited to all moving surfaces or plain trailing edge flaps. At each flight condition the six-body axis force and moment coefficients are provided. Both theoretical and empirical methods are included that encompass the entire speed regime from subsonic to hypersonic. Missile Datcom has been shown to provide very good agreement with experimental data for a variety of configurations. To validate the code for RLV type configurations, extensive comparisons

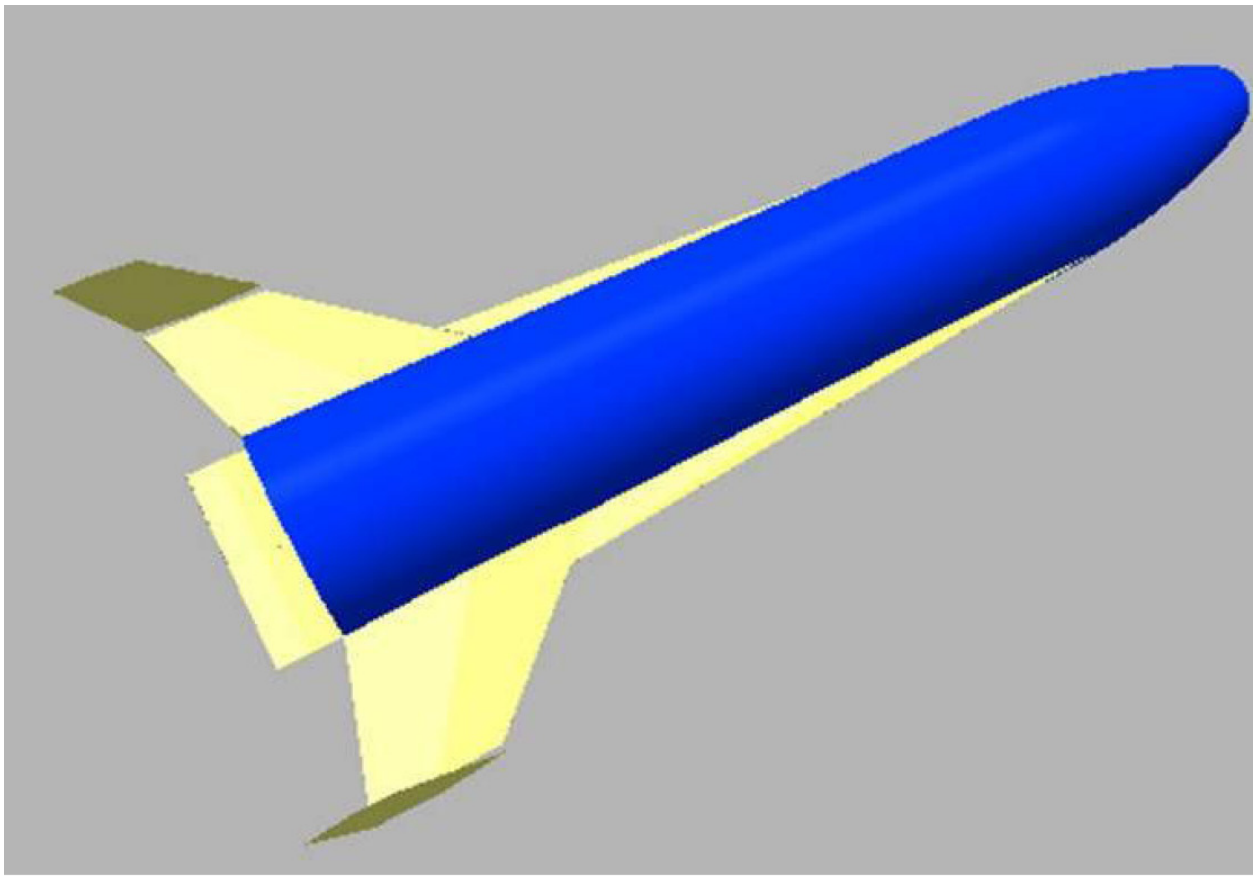

Figure 2. Preliminary Configuration for A Space Access Vehicle

have been made with wind tunnel data for the X-34 and X-40 configurations. Some of the X-34 comparisons are given by Ngo and Blake.[2]

Moments of inertia for the ARES vehicle were calculated using the following equations from Roskam:[3]

$$I_{xx} = \frac{W}{g}(k_x\, b)^2 \tag{1}$$

$$I_{yy} = \frac{W}{g}(k_y\, l)^2 \tag{2}$$

$$I_{zz} = \frac{W}{g}(k_z\, \frac{b+l}{2})^2 \tag{3}$$

The non-dimensional radii of gyration (k factors) were taken from an AFRL database of re-entry vehicle designs such as the Space Shuttle, X-40, etc.. Values used for k_x, k_y and k_z were 0.150, 0.25 and 0.30 respectively. This method does not give the product of inertia (I_{xz}) so this was assumed to be zero. The dimensions of the baseline space access vehicle design is summarized in Table 1. The control effectors limits

are shown in Table 2

Table 1. Space Access Vehicle Configuration Properties

Fuselage Length (feet)	Wing Span (feet)	Weight (pounds)	I_{xx} (slug-feet^2)	I_{yy} (slug-feet^2)	I_{zz} (slug-feet^2)	I_{xz} (slug-feet^2)
102	42	65,474	81,000	1,322,00	950,000	0

Table 2. Space Access Vehicle Control Effectors

Left Elevon	Right Elevon	Left Rudder	Right Rudder	Body Flap
$\pm$ 30°	$\pm$ 30°	$\pm$ 30°	$\pm$ 30°	$\pm$ 20°

III. DYNAMIC INVERSION

The inner-loop control architecture developed in this work consists of three major components: a dynamic inversion control law, a control allocation algorithm, and precompensation. The purpose of the inner-loop control system is to accurately track body-frame angular velocity vector commands. The goal of dynamic inversion in flight control is to cancel the wing-body-propulsion forces and moments with control effector forces and moments such that the vehicle can accurately track some desired commands. Dynamic inversion control laws[4] require the use of a control mixer or control effector allocation algorithm when the number of control effectors exceeds the number of controlled variables, or when actuator rate and position limits must be taken into account. It is quite common that the desired control variable rate commands can be achieved in many different ways and so control allocation algorithms are used to provide unique solutions to such problems.[?,5] The control allocation algorithm is significantly improved by including an intercept term.[6] To complete the inner-loop, precompensation blocks are designed to produce the desired closed-loop dynamics. For the purpose of demonstration, we develop a dynamic inversion control law for a vehicle with five control surfaces. The control surfaces include two rudders, two elevons, and a bodyflap. An outer-loop control system generates body-frame angular velocity commands (p_{des}, q_{des}, r_{des}), that the inner-loop dynamic inversion control system attempts to track. The dynamics of the body-frame angular velocity vector for this

vehicle can be written as

$$\dot{\boldsymbol{\omega}} = \mathbf{f}(\boldsymbol{\omega}, \mathbf{P}) + \mathbf{g}(\mathbf{P}, \boldsymbol{\delta}) \tag{4}$$

where $\boldsymbol{\omega} = [\text{p q r}]^T$, p, q, and r are the rolling, pitching, and yawing rates, respectively, $\mathbf{P}$ denotes measurable or estimable quantities that influence the body-frame states, and $\boldsymbol{\delta} = (\delta_1, \delta_2, \cdots, \delta_n)^T$ is a vector of control surface deflections. The vector $\mathbf{P}$ contains variables such as angle of attack, sideslip, Mach number, and vehicle mass properties. The term $\mathbf{g}(\mathbf{P}, \boldsymbol{\delta})$ includes the control dependent accelerations, while the term $\mathbf{f}(\boldsymbol{\omega}, \mathbf{P})$ describes accelerations that are due to the base-vehicle's (wing-body-propulsion) aerodynamic properties. The moment equations for a vehicle in the body-frame[7] can be manipulated to form control dependent and control independent terms. It is assumed that the mass properties of the vehicle under consideration are constant, thus, the time derivative of the inertia matrix can be set to zero, i.e., $\dot{\mathbf{I}} = \mathbf{0}$. Then, Equation 4 can be written as

$$\dot{\boldsymbol{\omega}} = \mathbf{I}^{-1}(\mathbf{G}_B(\boldsymbol{\omega}, \mathbf{P}, \boldsymbol{\delta}) - \boldsymbol{\omega} \times \mathbf{I}\boldsymbol{\omega}) \tag{5}$$

where

$$\begin{aligned} \mathbf{G}_B(\boldsymbol{\omega}, \mathbf{P}, \boldsymbol{\delta}) &= \mathbf{G}_{BAE}(\boldsymbol{\omega}, \mathbf{P}) + \mathbf{G}_\delta(\mathbf{P}, \boldsymbol{\delta}) \\ &= \begin{bmatrix} L \\ M \\ N \end{bmatrix}_{BAE} + \begin{bmatrix} L \\ M \\ N \end{bmatrix}_\delta \end{aligned} \tag{6}$$

In Equations 5 and 6, $\mathbf{I}$ is the inertia matrix and L, M, and N are the rolling, pitching, and yawing moments. In Equation 6, $\mathbf{G}_{BAE}(\boldsymbol{\omega}, \mathbf{P})$ is the moment generated by the base aerodynamic system (wing-body-propulsion system) and $\mathbf{G}_\delta(\mathbf{P}, \boldsymbol{\delta})$ is the sum of moments produced by the control effectors. Therefore,

$$\begin{aligned} \mathbf{f}(\boldsymbol{\omega}, \mathbf{P}) &= \mathbf{I}^{-1}[\mathbf{G}_{\mathbf{BAE}}(\boldsymbol{\omega}, \mathbf{P}) - \boldsymbol{\omega} \times \mathbf{I}\boldsymbol{\omega}] \\ \mathbf{g}(\mathbf{P}, \boldsymbol{\delta}) &= \mathbf{I}^{-1}\mathbf{G}_\delta(\mathbf{P}, \boldsymbol{\delta}) \end{aligned} \tag{7}$$

In order to utilize a linear control allocator, it is necessary that the control dependent portion of the model be linear in the controls. Hence, an affine approximation is developed such that

$$\mathbf{G}_\delta(\mathbf{P}, \boldsymbol{\delta}) \approx \widetilde{\mathbf{G}}_\delta(\mathbf{P})\boldsymbol{\delta} + \boldsymbol{\epsilon}(\mathbf{P}, \boldsymbol{\delta}) \tag{8}$$

The term $\boldsymbol{\epsilon}(\mathbf{P}, \boldsymbol{\delta})$ is an intercept term[6] for the body-axis angular accelerations which is used to improve the accuracy of linear control allocation algorithms. Using Equations 4, 7, and 8, the model used for the design of the dynamic inversion control law becomes

$$\dot{\boldsymbol{\omega}} = \mathbf{f}(\boldsymbol{\omega}, \mathbf{P}) + \mathbf{I}^{-1}\widetilde{\mathbf{G}}_{\delta}(\mathbf{P})\boldsymbol{\delta} + \mathbf{I}^{-1}\boldsymbol{\epsilon}(\mathbf{P}, \boldsymbol{\delta}) \tag{9}$$

The objective is to find a control law, that provides direct control over $\dot{\boldsymbol{\omega}}$, so that $\dot{\boldsymbol{\omega}} = \dot{\boldsymbol{\omega}}_{des}$. Hence, the inverse control law must satisfy

$$\begin{gathered} \dot{\boldsymbol{\omega}}_{des} - \mathbf{f}(\boldsymbol{\omega}, \mathbf{P}) - \mathbf{I}^{-1}\boldsymbol{\epsilon}(\mathbf{P}, \boldsymbol{\delta}) = \\ \mathbf{I}^{-1}\widetilde{\mathbf{G}}_{\delta}(\mathbf{P})\boldsymbol{\delta} \end{gathered} \tag{10}$$

Equation 10 provides the dynamic inversion control law for the body-frame angular velocity vector.

IV. CONTROL ALLOCATION

Since there are more control effectors than controlled variables and the control effectors are restricted by position and rate limits, a control allocation algorithm is necessary. For the lifting body under consideration, there are three controlled variables, namely, roll, pitch, and yaw rates, while there are five control surfaces (left and right rudders, left and right elevators, and a bodyflap). Hence, a control allocation scheme must be used to insure that Equation 10 is satisfied.

Control allocators are used in conjunction with some type of feedback control law whose output consists of one or more pseudo-control commands (typically desired moment or acceleration commands). The number of pseudo-control commands is always less than or equal to the number of control effectors. Dynamic inversion control laws and control allocation algorithms fit together quite naturally since the pseudo-control commands are easily identifiable. Also, it is quite common that the desired commands can be achieved in many different ways and so control allocation algorithms are used to provide unique solutions to such problems.

To begin development of the allocator, rewrite Equation 10 as

$$\begin{gathered} \mathbf{d}_{des} = \dot{\boldsymbol{\omega}}_{des} - \mathbf{f}(\boldsymbol{\omega}, \mathbf{P}) - \mathbf{I}^{-1}\boldsymbol{\epsilon}(\mathbf{P}, \boldsymbol{\delta}) = \\ \mathbf{I}^{-1}\widetilde{\mathbf{G}}_{\delta}(\mathbf{P})\boldsymbol{\delta} = \mathbf{B}\boldsymbol{\delta} \end{gathered} \tag{11}$$

where $\mathbf{d}_{des}$ are the body-axis accelerations that need to be produced by the control effectors and $\mathbf{B}$ is the

control effectiveness matrix defined as

$$\mathbf{B} = \mathbf{I}^{-1}\widetilde{\mathbf{G}}_{\delta}(\mathbf{P}) = \mathbf{I}^{-1}\begin{bmatrix} \frac{\partial L}{\partial \delta_1} \frac{\partial L}{\partial \delta_2} \cdots \frac{\partial L}{\partial \delta_n} \\ \\ \frac{\partial M}{\partial \delta_1} \frac{\partial M}{\partial \delta_2} \cdots \frac{\partial M}{\partial \delta_n} \\ \\ \frac{\partial N}{\partial \delta_1} \frac{\partial N}{\partial \delta_2} \cdots \frac{\partial N}{\partial \delta_n} \end{bmatrix} \tag{12}$$

The control allocation objective, in the linear case, is to find $\boldsymbol{\delta}$ such that

$$\mathbf{d}_{des} = \mathbf{B}\boldsymbol{\delta} \tag{13}$$

subject to rate and position limits on the control effectors. Notice that Equation 13 defines a linear subspace in the $(\mathbf{d}_{des}, \boldsymbol{\delta})$ space.

Equation 13 can be posed as the following optimization problem:

$$\min_{\delta} J_E = \min_{\delta} \|\mathbf{B}\boldsymbol{\delta} - \mathbf{d}_{des}\|_1 \tag{14}$$

subject to

$$\overline{\boldsymbol{\delta}} \leq \boldsymbol{\delta} \leq \underline{\boldsymbol{\delta}} \tag{15}$$

where J_E is the performance index for the error minimization problem, $\underline{\boldsymbol{\delta}}$, $\overline{\boldsymbol{\delta}}$ are the most restrictive lower and upper limits on the control effectors, respectively and the 1-norm is selected so that linear programming techniques can be used to solve the problem.[8] More specifically,

$$\begin{aligned} \overline{\boldsymbol{\delta}} &= \min(\boldsymbol{\delta}_U, \boldsymbol{\delta} + \dot{\boldsymbol{\delta}}\Delta t) \\ \underline{\boldsymbol{\delta}} &= \max(\boldsymbol{\delta}_L, \boldsymbol{\delta} - \dot{\boldsymbol{\delta}}\Delta t) \end{aligned} \tag{16}$$

where $\boldsymbol{\delta}_L, \boldsymbol{\delta}_U$ are the lower and upper position limits, $\boldsymbol{\delta}$ is the current location of the control effectors, $\dot{\boldsymbol{\delta}}$ is a vector of rate limits, and Δt is the timestep or control update rate.

If sufficient control authority exists such that J_E can be made identically equal to zero, then it may be possible to optimize a sub-objective. This optimization problem can be posed as follows:

$$\min_{\delta} J_C = \min_{\delta} \|\mathbf{W}_{\delta}(\boldsymbol{\delta} - \boldsymbol{\delta}_p)\|_1 \tag{17}$$

subject to

$$\begin{aligned} \mathbf{B}\boldsymbol{\delta} &= \mathbf{d}_{des} \\ \overline{\boldsymbol{\delta}} &= \min(\boldsymbol{\delta}_U, \boldsymbol{\delta} + \dot{\boldsymbol{\delta}}\Delta t) \\ \underline{\boldsymbol{\delta}} &= \max(\boldsymbol{\delta}_L, \boldsymbol{\delta} - \dot{\boldsymbol{\delta}}\Delta t) \end{aligned} \tag{18}$$

where $\mathbf{W}_\delta$ is a weighting matrix and $\boldsymbol{\delta}_p$ is a preferred set of control effector deflections. The problem posed in Equation 17 is termed the control minimization problem.

In practice, the two optimization problems given in Equations 14 and 17 are combined to form what is known as the mixed optimization problem. The mixed optimization problem is defined as

$$\begin{aligned} &\min_{\delta} J_M = \\ &\min_{\delta} \left(\|\mathbf{B}\boldsymbol{\delta} - \mathbf{d}_{des}\|_1 + \lambda \|\mathbf{W}_\delta(\boldsymbol{\delta} - \boldsymbol{\delta}_p)\|_1 \right) \end{aligned} \tag{19}$$

where the parameter λ is used to weight the error and control minimization problems. For this work, it was determined that $\lambda = 0.01$ provided good error minimization while still driving the control effectors to the preferred values when sufficient control authority existed. The advantage of the mixed optimization problem is that it can often be solved faster and with better numerical properties as compared to sequentially solving the error and control minimization problems.[5]

A. Control Allocation Preference Vector and Effector Failures

As specified in Equation 19, a preference vector, $\boldsymbol{\delta}_p$, must be selected. One difficulty with the linear programming framework for solving the control allocation problem is that no model of the control allocator exists. This causes problems when performing linear stability analysis as there is no way to know the input/output relationship of the allocation algorithm. Fortunately, when sufficient control authority exists, the allocation algorithm will attempt to minimize the difference between the control deflections and a preferred set of control deflections. One obvious choice for preference vector is the pseudo-inverse solution. In this case, when sufficient control authority exists, the control allocation algorithm will drive the surfaces to the pseudo-inverse solution. Hence, in a robustness analysis, the control allocator can be replaced by the pseudo-inverse solution (assuming sufficient control authority exists). The pseudo-inverse solution is the two-norm solution to the control allocation problem and can be formulated as follows:

$$\min_{\boldsymbol{\delta}} \frac{1}{2}(\boldsymbol{\delta} + \mathbf{c})^{\mathbf{T}}\mathbf{W}(\boldsymbol{\delta} + \mathbf{c}) \tag{20}$$

subject to

$$\mathbf{B}\boldsymbol{\delta} = \mathbf{d}_{des} \tag{21}$$

where $\mathbf{W}$ is a weighting matrix and $\mathbf{c}$ is an offset vector. To solve this problem, first find the Hamiltonian (H) such that

$$\begin{aligned} H = \frac{1}{2}\boldsymbol{\delta}^T\mathbf{W}\boldsymbol{\delta} + \frac{1}{2}\mathbf{c}^T\mathbf{W}\boldsymbol{\delta} + \\ \frac{1}{2}\boldsymbol{\delta}^T\mathbf{W}\mathbf{c} + \frac{1}{2}\mathbf{c}^T\mathbf{W}\mathbf{c} + \boldsymbol{\xi}(\mathbf{B}\boldsymbol{\delta} - \mathbf{d}_{des}) \end{aligned} \tag{22}$$

where $\boldsymbol{\xi} \in \mathbb{R}^n$ is an as yet undetermined Lagrange multiplier. Taking the partial derivatives of H with respect to $\boldsymbol{\delta}$ and $\boldsymbol{\xi}$, setting these expressions equal to zero, and rearranging, gives

$$\begin{aligned} \frac{\partial H}{\partial \boldsymbol{\delta}} &= \mathbf{W}\boldsymbol{\delta} + \frac{1}{2}(\mathbf{c^T W})^T + \\ &\quad \frac{1}{2}\mathbf{W}\mathbf{c} + (\boldsymbol{\xi}\mathbf{B})^T = \mathbf{0} \\ \implies \mathbf{W}\boldsymbol{\delta} &= -\mathbf{W}\mathbf{c} - \mathbf{B^T}\boldsymbol{\xi}^\mathbf{T} \end{aligned} \tag{23}$$

and

$$\begin{aligned} \frac{\partial H}{\partial \boldsymbol{\xi}} &= \mathbf{B}\boldsymbol{\delta} - \mathbf{d}_{des} = \mathbf{0} \\ \implies \mathbf{B}\boldsymbol{\delta} &= \mathbf{d}_{des} \\ \implies \mathbf{B}\mathbf{W}^{-1}\mathbf{W}\boldsymbol{\delta} &= \mathbf{d}_{des} \end{aligned} \tag{24}$$

Substituting Equation 23 into Equation 24 yields

$$\mathbf{B}\mathbf{W}^{-1}[-\mathbf{W}\mathbf{c} - \mathbf{B}^T\boldsymbol{\xi}^T] = \mathbf{d}_{des} \tag{25}$$

Solving for $\boldsymbol{\xi}^T$ in Equation 25 yields

$$\boldsymbol{\xi}^T = -(\mathbf{B}\mathbf{W}^{-1}\mathbf{B}^T)^{-1}[\mathbf{d}_{des} + \mathbf{B}\mathbf{c}] \tag{26}$$

Substituting Equation 26 into Equation 23 produces

$$\mathbf{W}\boldsymbol{\delta} = -\mathbf{W}\mathbf{c} + \mathbf{B}^T(\mathbf{B}\mathbf{W}^{-1}\mathbf{B}^T)^{-1}[\mathbf{d}_{des} + \mathbf{B}\mathbf{c}] \tag{27}$$

Simplifying Equation 27 gives the desired result

$$\begin{aligned} \boldsymbol{\delta} = \boldsymbol{\delta}_p = \\ -\mathbf{c} + \mathbf{W}^{-1}\mathbf{B}^T(\mathbf{B}\mathbf{W}^{-1}\mathbf{B}^T)^{-1}[\mathbf{d}_{des} + \mathbf{B}\mathbf{c}] \end{aligned} \tag{28}$$

Equation 28 gives the pseudo-inverse solution. It should be noted that if an effector is offset, two items must be taken into account, position offset ($-\mathbf{c}$) and the moments generated by the offset ($\mathbf{Bc}$). For the specific usage of the pseudo-inverse control allocation solution, the weighting matrix was selected to be diagonal, such that,

$$\mathbf{W} = diag \\ [W_{\delta_{RF}}\ W_{\delta_{LF}}\ W_{\delta_{RR}}\ W_{\delta_{LR}}\ W_{\delta_{SB}}\ W_{\delta_{BF}}] \tag{29}$$

where 'diag' represents a diagonal matrix with the entries along the main diagonal being the weights associated with each control effector.

This control allocation formulation allows one to simulate a control effector failure rather easily. A failure is introduced by simply setting the lower and upper positions limits on the effected control surface equal to each other. For a failed control surface, its effects must also be accounted for in the pseudo-inverse preference vector, which requires two modifications. First, the location of the failure must be inserted into the offset vector. Here, the appropriate component of $\mathbf{c}$ is set to the negative of the failure position. Second, the appropriate entry in the weighting matrix, $\mathbf{W}$, needs to be increased. Nominally, the entries in $\mathbf{W}$ are one and an increase in the value will place more penalty on usage of that particular surface.

V. Guidance Loops

The guidance loops developed in this work have as inputs angle of attack error α_e and euler angle phi error ϕ_e and provide as outputs the commanded roll, pitch, and yaw rates. A backstepping approach is used to move from the angle of attack and phi loops to the body-axis rate loops.

To derive the pitch rate command, the governing equation of motion is

$$\gamma = \theta - \alpha \tag{30}$$

Therefore,

$$\dot{\alpha} = \dot{\theta} - \dot{\gamma} \tag{31}$$

By definition,

$$\dot{\theta} = q\cos\phi - r\sin\phi \tag{32}$$

and

$$\dot{\gamma} = \frac{L}{mV} - \frac{g}{V}\cos\gamma \tag{33}$$

where L is the total vehicle lift, m is the mass, V is the velocity, and g is the acceleration due to gravity. Substituting Eqs. 32 and 33 into Eq. 31 yields

$$\dot{\alpha} = q\cos\phi - r\sin\phi - \frac{L}{mV} + \frac{g}{V}\cos\gamma \tag{34}$$

From dynamic inversion, the pitch rate command becomes

$$q_{des} = \sec\phi\left(\dot{\alpha}_{des} + r\sin\phi + \frac{L}{mV} - \frac{g}{V}\cos\gamma\right) \tag{35}$$

The desired angle of attack dynamics are defined by the following proportional-integral control on α error:

$$\dot{\alpha}_{des} = \left(k_{p_\alpha} + \frac{k_{i_\alpha}}{s}\right)(\alpha_{des} - \alpha) \tag{36}$$

For the lateral channels, the roll rate command is simply the result of a proportional-integral operation on phi error. Thus,

$$p_{des} = \left(k_{p_\phi} + \frac{k_{i_\phi}}{s}\right)(\phi_{des} - \phi) \tag{37}$$

From the coordinated turn equations, the yaw rate command is computed using

$$r_{des} = p\tan\alpha + \frac{g}{U}\sin\phi \tag{38}$$

Equations 37, 35, and 38 define the commanded or desired body axis rates generated from errors between the actual and desired angle of attack α_{des} and desired roll angle ϕ_{des}.

VI. RESULTS

In this section, we will use the above aforementioned methods to obtain a guidance and control law for a space vehicle undergoing a preliminary design evaluation. Given a reentry trajectory, a POST simulation outputs the desired angle of attack α_{des} and desired roll angle ϕ_{des} as part of its calculations. A guidance law based on the backstepping method discussed in section V is designed to convert the desired angle of attack α_{des} and desired roll angle ϕ_{des} into the commanded roll rate P_{comd}, the commanded pitch rate Q_{comd} and the commanded yaw rate R_{comd}. The commanded body-axis rates P_{comd}, Q_{comd}, R_{comd}, in turn, are converted into required control deflections by a dynamic-inversion control law mentioned in section III.

A control allocator based on the discussion in section IV assigns the required control deflections over the control effectors according to their available capabilities. The tracking performance of the control law is shown in Figure 3. Tracking errors $P_{comd} - P_{actual}$, $Q_{comd} - Q_{actual}$, $R_{comd} - R_{actual}$ are small. These small errors are desired and expected since our design method is formulated to directly track P_{comd}, Q_{comd}, R_{com}. The simulation performed in POST does not include the impact of additional drag associated the control effectors activities in trimming the vehicle and tracking the given trajectory, differences between the actual roll, pitch, and yaw angles and those calculated by POST as shown in Figure 4. In Figures 5 and 6 the deflection activities of the left elevon, right elevon, left rudder and right rudder are reasonable without exceeding its rate and position limits. It is noted, however, that the pitch flap briefly saturates in its deflection limit. For a given trajectory, it is not desirable for any control effector to experience either a rate or a position saturation under a nominal condition. To avoid control saturation, there are many options ranging from hardware considerations, to software modifications, to trajectory planning. In the next discussion, we will examine how the issue can be addressed from the point of view of stability and control namely control sizing, and center of gravity location.

A. Aero-Control Surface Resizing

As seen in Figure 5 the body flap experiences saturation. By enlarging this control effector, it is hoped the saturation can be avoided. For this study, the cord of the body flap is increased by 40% from its baseline of 5 feet to 7 feet. The control activities of the body flap is seen in Figure 8 The body flap still experiences saturation. At this stage of the design, other changes on the vehicle can be experimented to affect the vehicle's stability and control such as moving the vehicle's center of gravity, reducing its strakes.

VII. CONCLUSIONS

In this work, a rapid assessment tool for space access vehicle configurations in guidance and control performance was presented. The reentry trajectory was found using a well-known, high-fidelity trajectory generator. To track this trajectory, an inner-loop control law was designed for a reentry vehicle with five control surfaces. The control law utilized a dynamic inversion controller and a linear programming based control allocation algorithm. Evaluation of the vehicle's guidance and control performance showed that the

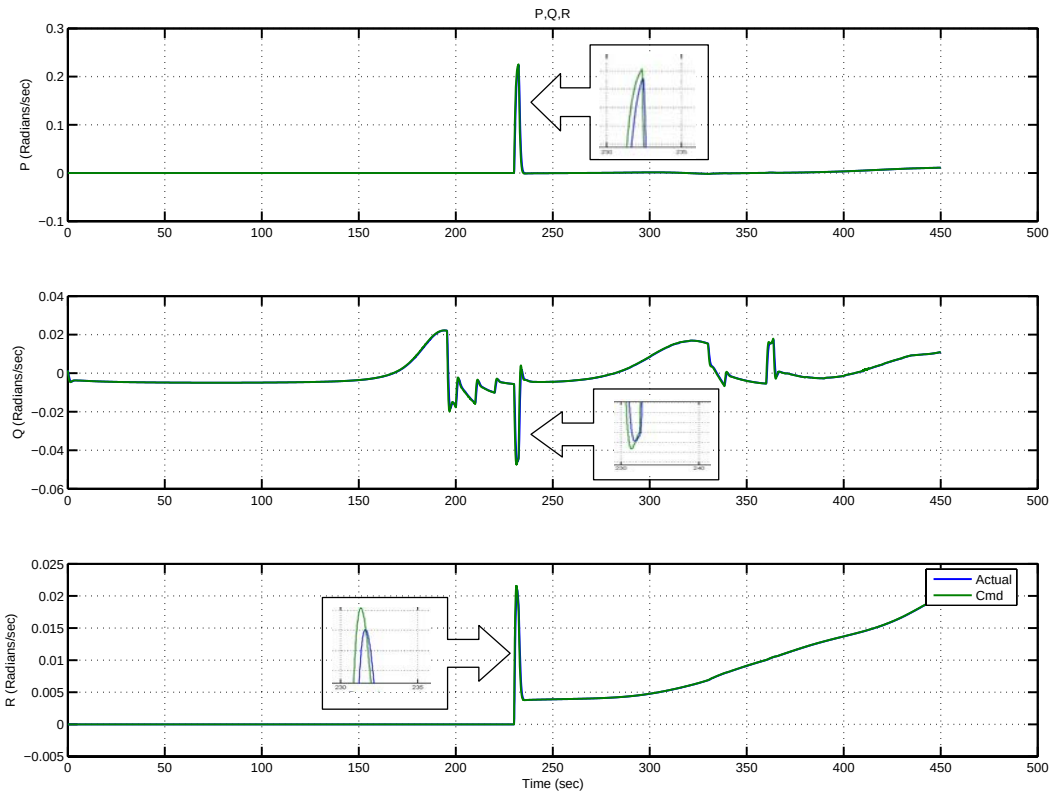

Figure 3. Pitch Rate, Roll Rate, and Yaw Rate Tracking

body flap experienced deflection saturation during a nominal reentry flight. It is thus necessary to consider modifications of the vehicle such as control surface sizing, moving the vehicle's center of gravity, resizing the wing, strake areas. Using the tool detailed in this paper, such modifications of the vehicle can be accommodated during the early design stages to incorporate the guidance and control requirements

References

[1]Blake, W. B., "Missile Datcom User's Manual - 1997 FORTRAN 90 Revision," Tech. Rep. VA-WP-TR-1998-3009, AFRL, WPAFB, OH, Aug. 1998.

[2]Ngo, A. D. and Blake, W. B., "Longitudinal Control and Footprint Analysis for a Reusable Military Launch Vehicle ," *Proceedings of the 2003 AIAA Guidance Navigation and Control Conference*, AIAA 2003-5738, August 2003.

[3]Roskam, J., *Airplane Design*, Roskam Aviation & Engineering Corporation, 1989.

[4]"Application of Multivariable Control Theory to Aircraft Control Laws," Tech. Rep. WL-TR-96-3099, Wright Laboratory,

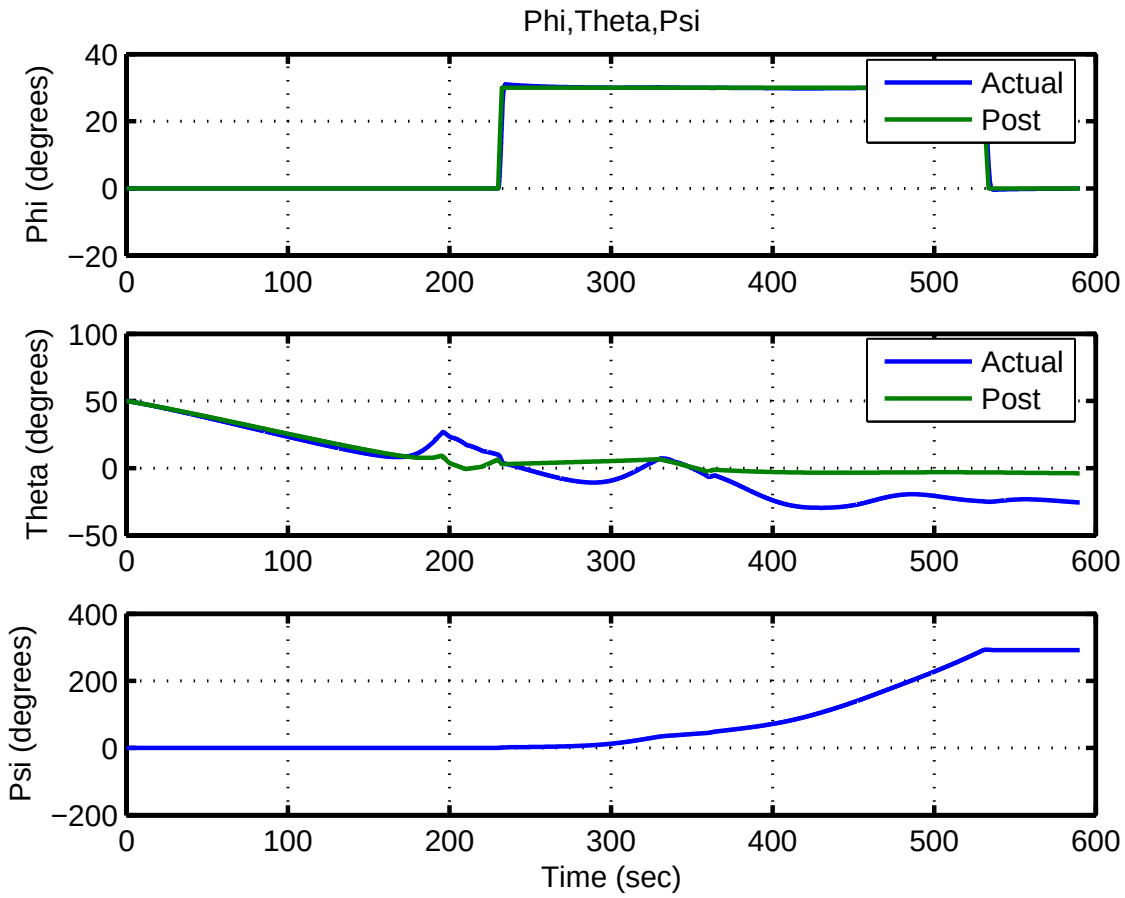

Figure 4. Rolling Angle, Pitch Angle, and Yaw Angle Tracking

WPAFB, OH, 1996.

[5]Bodson, M., "Evaluation of Optimization Methods for Control Allocation," *Journal of Guidance, Control and Dynamics*, Vol. 25, No. 4, 2002, pp. 703–711.

[6]Doman, D. B. and Oppenheimer, M. W., "Improving Control Allocation Accuracy for Nonlinear Aircraft Dynamics," *Proceedings of the 2002 Guidance, Navigation and Control Conference*, AIAA 2002-4667, August 2002.

[7]Etkin, B., *Dynamics of Atmospheric Flight*, John Wiley & Sons, Inc., 1972.

[8]Buffington, J. M., " Modular Control Law Design for the Innovative Control Effectors (ICE) Tailless Fighter Aircraft Configuration 101-3," Tech. Rep. AFRL-VA-WP-TR-1999, Air Force Research Laboratory, Wright-Patterson A.F.B., OH, 1999, pp 93-94.

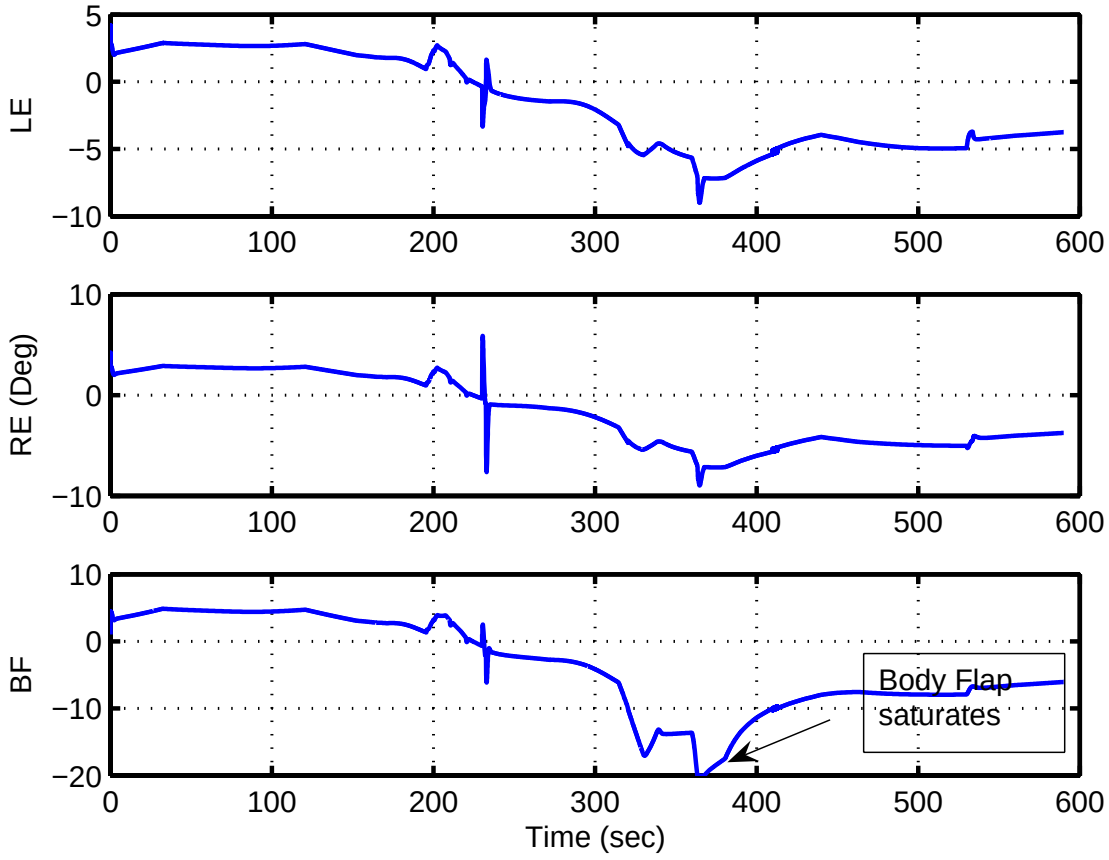

Figure 5. Left Elevon, Righ Elevon, Body Flap Deflections

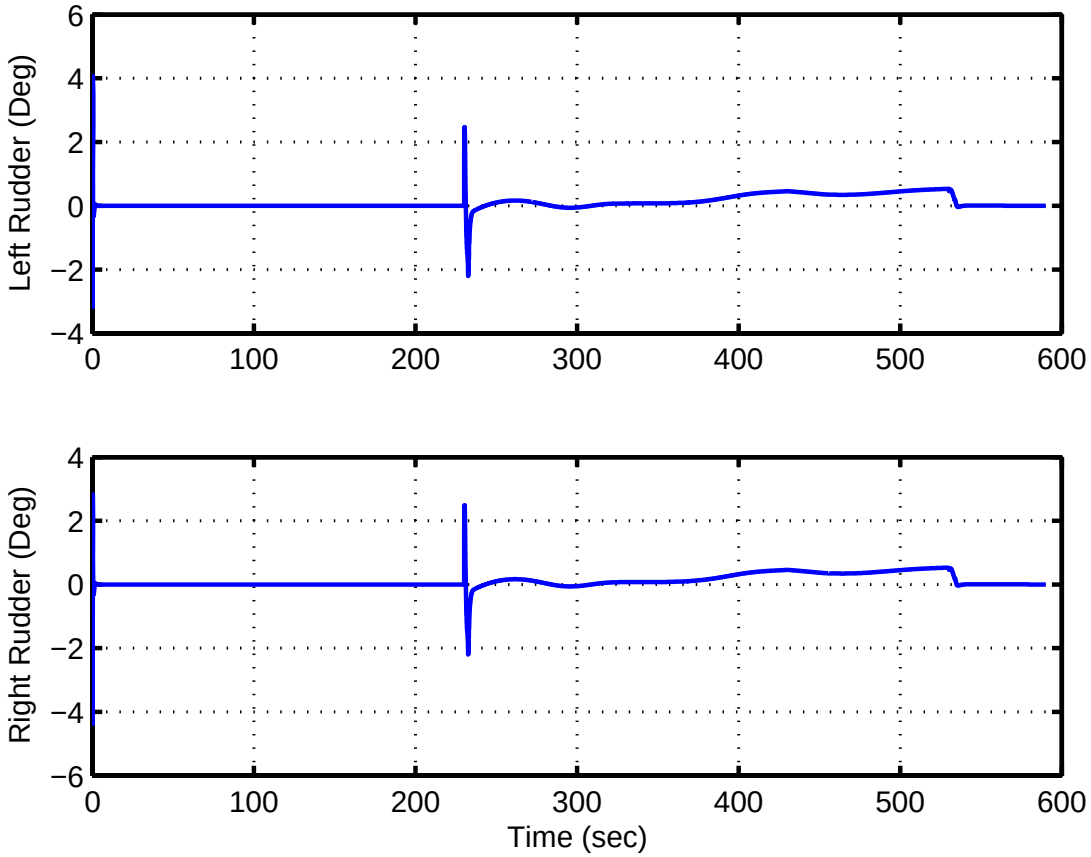

Figure 6. Left Rudder, Righ Rudder Deflections

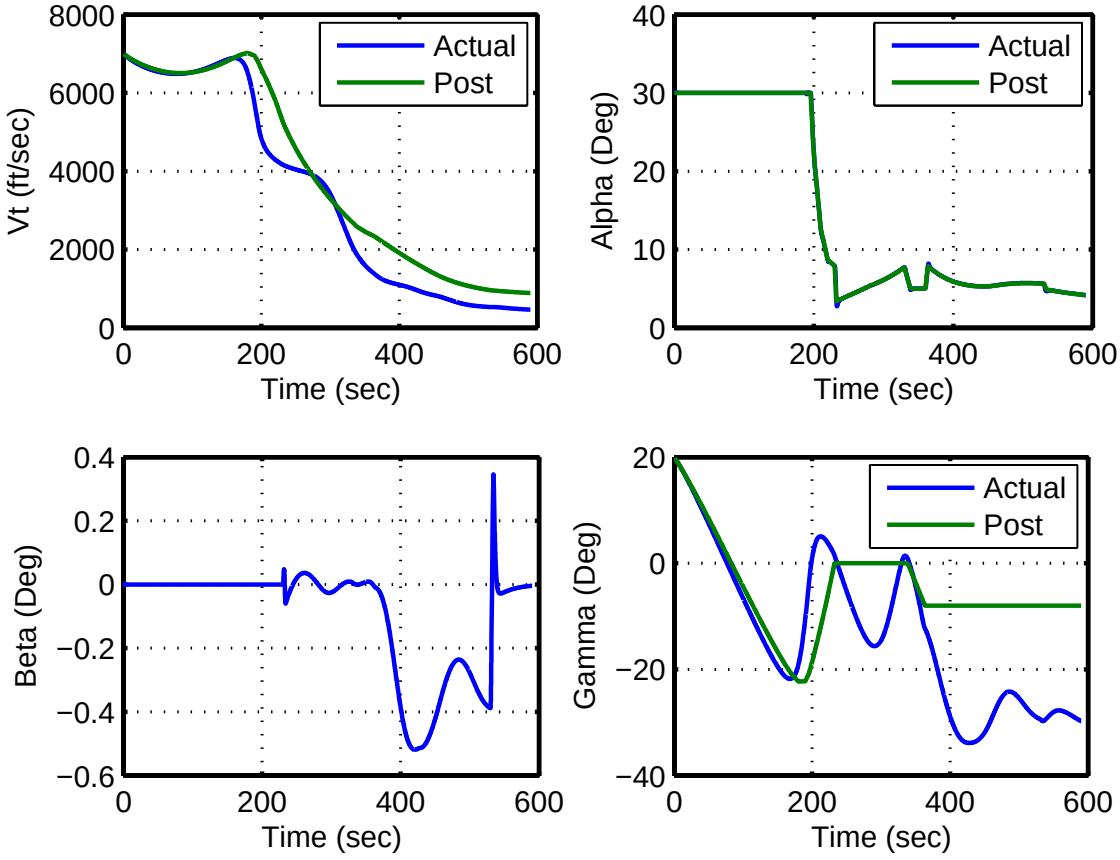

Figure 7. Velocity, Angle of Attack, Side Slip Angle, and Flight Path Angle Tracking

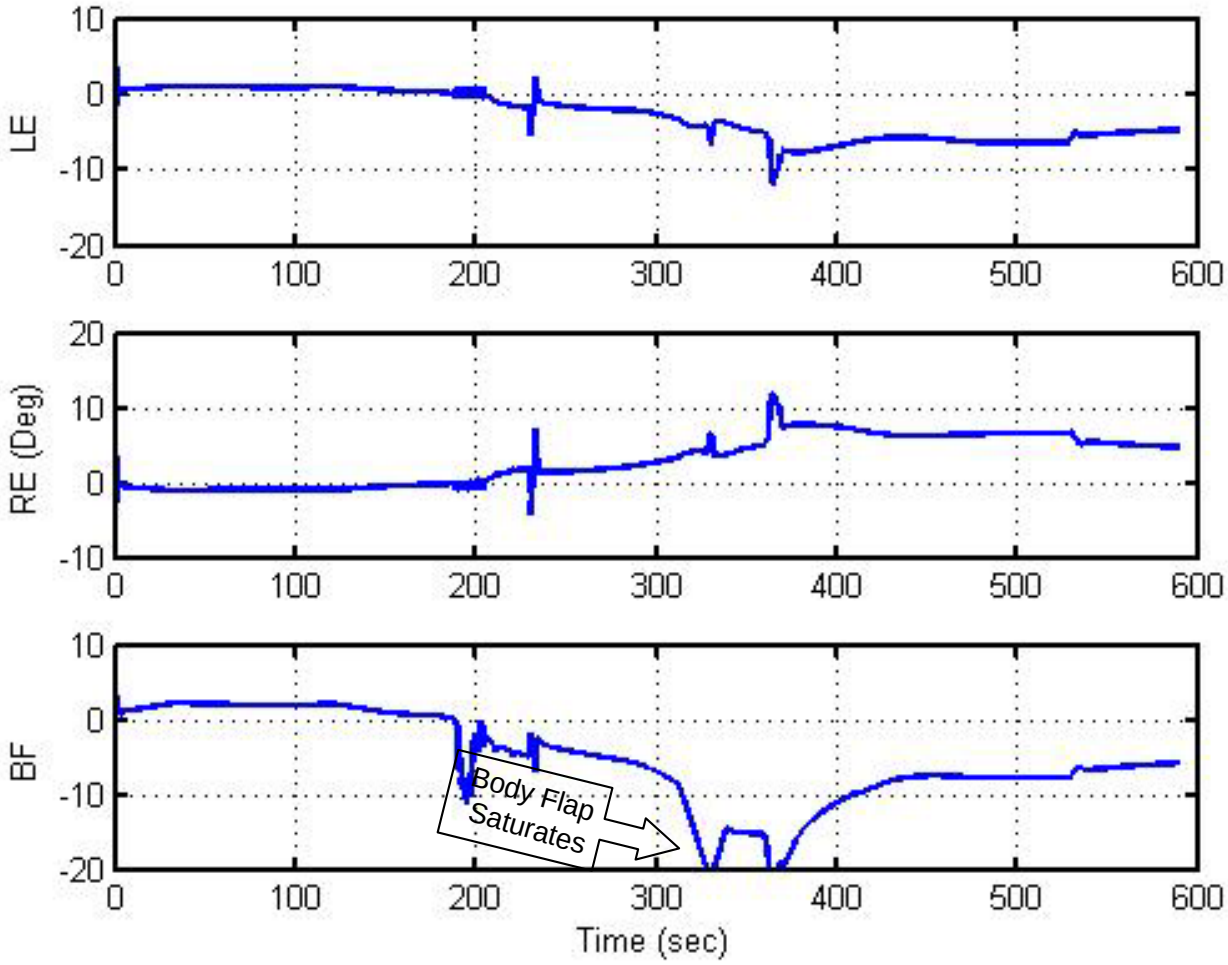

Figure 8. Left Elevon, Righ Elevon, Body Flap Deflections